Hyaluronan and CD44 antagonize mitogen-dependent cyclin D1 expression in mesenchymal cells

Devashish Kothapalli,[1] Liang Zhao,[3] Elizabeth A. Hawthorne,[1] Yan Cheng,[1,2] Eric Lee,[3] Ellen Puré,[1,2,3,4] and Richard K. Assoian[1,2,3]

[1]Department of Pharmacology and [2]Institute for Translational Medicine and Therapeutics, University of Pennsylvania School of Medicine, Philadelphia, PA 19104
[3]Wistar Institute, Philadelphia, PA 19104
[4]Ludwig Institute for Cancer Research, New York, NY 10158

High molecular weight (HMW) hyaluronan (HA) is widely distributed in the extracellular matrix, but its biological activities remain incompletely understood. We previously reported that HMW-HA binding to CD44 antagonizes mitogen-induced S-phase entry in vascular smooth muscle cells (SMCs; Cuff, C.A., D. Kothapalli, I. Azonobi, S. Chun, Y. Zhang, R. Belkin, C. Yeh, A. Secreto, R.K. Assoian, D.J. Rader, and E. Puré. 2001. *J. Clin. Invest.* 108:1031–1040); we now characterize the underlying molecular mechanism and document its relevance in vivo. HMW-HA inhibits the mitogen-dependent induction of cyclin D1 and down-regulation of $p27^{kip1}$ in vascular SMCs. $p27^{kip1}$ messenger RNA levels were unaffected by HMW-HA, but the expression of Skp2, the rate-limiting component of the SCF complex that degrades $p27^{kip1}$, was reduced. Rescue experiments identified cyclin D1 as the primary target of HMW-HA. Similar results were observed in fibroblasts, and these antimitogenic effects were not detected in CD44-null cells. Analysis of arteries from wild-type and CD44-null mice showed that the effects of HMW-HA/CD44 on cyclin D1 and Skp2 gene expression are detected in vivo and are associated with altered SMC proliferation after vascular injury.

Introduction

Hyaluronan (HA) is a glycosaminoglycan that is broadly distributed in extracellular spaces (Aruffo et al., 1990). HA is especially enriched in pericellular matrices surrounding migrating and proliferating cells during embryonic development, tissue repair, and inflammation (Fraser et al., 1997). The most widely distributed form of HA in normal tissues is a high molecular weight (HMW) extracellular and cell surface polysaccharide that usually consists of several million daltons (called HMW-HA). HMW-HA forms a highly viscous network that is important for molecular exclusion, flow resistance, tissue osmosis, lubrication, and hydration. Lower molecular weight forms of HA that are synthesized de novo or generated by either hyaluronidase-mediated degradation or oxidative hydrolysis of HMW-HA may accumulate at sites of inflammation (Hawkins and Davies, 1998; Noble, 2002). The biological activities of HMW-HA and the lower molecular weight forms of HA are distinct (Cuff et al., 2001; Puré and Cuff, 2001; Noble, 2002).

HMW-HA and lower molecular weight forms of HA influence proliferation, migration, and adhesion of cells within matrices by binding to cell surface receptors such as CD44, RHAMM, LYVE-1, and layilin (Turley et al., 1987; Banerji et al., 1999; Bono et al., 2001). CD44, which is arguably the best studied HA receptor, is a type I transmembrane glycoprotein encoded by a single gene and expressed as multiple isoforms. The structural diversity of CD44 is generated by alternative RNA splicing as well as differential posttranslational modifications, including glycosylation and the attachment of glycosaminoglycans (Brown et al., 1991; Stamenkovic et al., 1991; Greenfield et al., 1999). The HA-binding domain is present in all isoforms of CD44. We previously reported that HMW-HA and a lower molecular weight HA regulate cell cycle progression through G1 phase in vascular smooth muscle cells (SMCs; Cuff et al., 2001). Interestingly, SMCs treated with HMW-HA were blocked in G1 phase, whereas the lower molecular form of

Correspondence to Richard K. Assoian: rka@pharm.med.upenn.edu

Abbreviations used in this paper: cdk, cyclin-dependent kinase; HA, hyaluronan; HMW, high molecular weight; MEF, mouse embryonic fibroblast; QPCR, quantitative PCR; SMC, smooth muscle cell.

The online version of this article contains supplemental material.

The Journal of Cell Biology, Vol. 176, No. 4, February 12, 2007 535–544
http://www.jcb.org/cgi/doi/10.1083/jcb.200611058

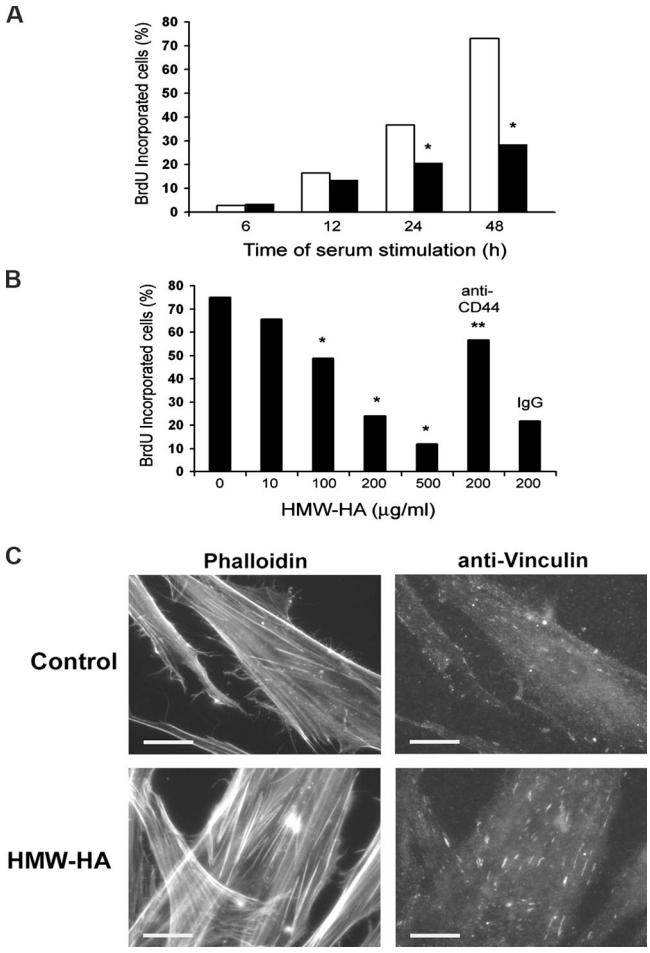

Figure 1. **HMW-HA inhibits S-phase entry in human SMCs.** (A) Quiescent human vascular SMCs were stimulated with 10% FBS for the selected times in the absence (control; white bars) or presence (black bars) of 200 μg/ml HMW-HA. *, $P < 0.001$. (B) Quiescent human vascular SMCs were stimulated with 10% FBS for 48 h in the presence of increasing concentrations of HMW-HA. A blocking antibody specific for human CD44 (5F12) or 50 μg/ml of an isotype-matched irrelevant antibody was added to the cells at the time of FBS stimulation and remained in the culture for the duration of the experiment. BrdU incorporation into nuclei was determined by immunofluorescence microscopy. *, $P < 0.01$; **, $P < 0.001$. (C) Quiescent human SMCs were stimulated with 10% FBS in the presence or absence of 200 μg/ml HMW-HA for 24 h. The cells were then stained with fluorescein-phalloidin and antivinculin. FBS-stimulated BrdU incorporation was inhibited 54% by HMW-HA in this experiment. Bars, 20 μm.

HA ($M_r = \sim 2 \times 10^5$) stimulated progression through G1 phase (Cuff et al., 2001). CD44 was required for both of these effects (Cuff et al., 2001).

Progression through G1 phase is regulated by cyclin-dependent kinases (cdks), cyclin D–cdk4 or cdk6 (hereafter called cdk4/6), and cyclin E–cdk2. Once activated, these cdks phosphorylate pocket proteins such as Rb (retinoblastoma) and p107, leading to the release of E2Fs and E2F-dependent gene transcription. E2F regulates several genes that are needed for the entry and completion of S phase as well as for further cell cycle progression (Dimova and Dyson, 2005). Mitogenic stimulation activates cdk4/6 by allowing for the induction of at least one member of the cyclin D family (D1, D2, or D3), with D1 being a major D-type cyclin in mesenchymal cells such as fibroblasts and vascular SMCs. The mechanisms leading to the mitogen-dependent activation of cyclin E–cdk2 are more complex, involving decreases in the expression of p21 family cdk inhibitors ($p21^{cip1}$, $p27^{kip1}$, and $p57^{kip2}$). $p21^{cip1}$ and $p27^{kip1}$ (hereafter called p21 and p27) are the best characterized. These inhibitors bind to cyclin E–cdk2 complexes in G0 and early G1 phases to maintain them in a catalytically inactive state (Sherr and Roberts, 1999). The down-regulation of p21 and p27 in late G1 phase contributes to the late G1-phase activation of cyclin E–cdk2. In addition, the p21 family cdk inhibitors promote the assembly (Sherr and Roberts, 1999) or stability (Bagui et al., 2003) of cyclin D–cdk4/6 complexes without inhibiting their catalytic activity. In fact, the mitogen-dependent induction of cyclin D1 is thought to contribute to the activation of cyclin E–cdk2 indirectly by sequestering p21/p27 on cyclin D–cdk4/6 complexes and, thereby, preventing p21/p27 from inhibiting cyclin E–cdk2 (Sherr and Roberts, 1999).

This study was designed to identify the cell cycle regulatory mechanism responsible for the antimitogenic effect of HMW-HA in vascular SMCs, to determine the applicability of the mechanism to other mesenchymal cell types, and to assess the relevance of the mechanism during SMC proliferation in vivo. We conclude that HMW-HA binding to CD44 selectively inhibits cyclin D1 expression and p27 degradation in both vascular SMCs and fibroblasts. The effect on cyclin D1 is primary, whereas the effect on p27 is caused by an HA/cyclin D1–dependent inhibition of Skp2, the rate-limiting component of the SCF^{Skp2} complex that degrades p27. These effects can account for the antimitogenic effect of HMW-HA on S-phase entry in vitro, are detected in vivo, and are associated with increased SMC proliferation after vascular injury in CD44-null mice.

Results

HMW-HA inhibits Rb hyperphosphorylation and cyclin A expression in human vascular SMCs

We previously reported that HMW-HA inhibits the S-phase entry of mouse vascular SMCs (Cuff et al., 2001). A similar antimitogenic effect was detected in early passage human vascular SMCs, as determined by BrdU labeling (Fig. 1 A) and flow cytometry (Table I). The effect was dose dependent and was largely reversed by anti-CD44 but not by an isotype-matched irrelevant antibody (Fig. 1 B). The small antimitogenic HMW-HA effect remaining in human vascular SMCs treated with neutralizing anti-CD44 may be caused by the actions of alternative HA receptors (see Introduction).

Other ECM components with antimitogenic activity (e.g., the matricellular proteins thrombospondin, SPARC [secreted protein acidic rich in cysteine], and tenascin-C) disassemble focal adhesions, disrupt actin stress fibers, and can also inhibit cell spreading (Bradshaw and Sage, 2001; Murphy-Ullrich, 2001). HMW-HA had none of these effects even under conditions in which it showed its typical inhibitory effect on S-phase entry (Fig. 1 C).

Table I. **HA inhibits S-phase entry in human and mouse SMCs**

Cell cycle phase	Percentage	
	mSMC	hSMC
Serum starved		
G0/G1	91	84
S	3	6
G2/M	5	3
FBS (24 h)		
G0/G1	59	84
S	18	11
G2/M	23	2
FBS (24 h) + HMW-HA		
G0/G1	89	94
S	4	3
G2/M	3	3

Quiescent human SMCs (hSMCs) and mouse SMCs (mSMCs) were stimulated with 10% FBS for 24 h in the absence or presence of 200 μg/ml HMW-HA. Cells were collected, washed with PBS, fixed in ethanol, stained with propidium iodide, and analyzed for DNA content by flow cytometry using standard procedures. Results show the percentages of cells in different stages of the cell cycle.

We explored the mechanism underlying the CD44-dependent antimitogenic effect of HMW-HA by examining hyperphosphorylation of the Rb protein and induction of cyclin A, which are two cell cycle events that are closely linked to the completion of G1 phase and entry into S phase. HMW-HA blocked the mitogen-dependent hyperphosphorylation of Rb (shown by the gel shift; Fig. 2 A). Rb hyperphosphorylation results in the release of activator E2Fs and E2F-dependent gene transcription, and cyclin A is one of the E2F-regulated genes. Indeed, cyclin A promoter activity was inhibited by HMW-HA (Fig. 2 B). Moreover, the expression of human papillomavirus E7, which inactivates pocket proteins and results in E2F release, rescued cyclin A promoter activity in HMW-HA–treated SMCs (Fig. 2 B), demonstrating that the inhibitory effect of HMW-HA on the cyclin A promoter is directly related to its effect on pocket protein phosphorylation. Consistent with its effect on the cyclin A promoter, HMW-HA inhibited the mitogen-dependent induction of cyclin A mRNA (Fig. 2 C) and protein (Fig. 3 A).

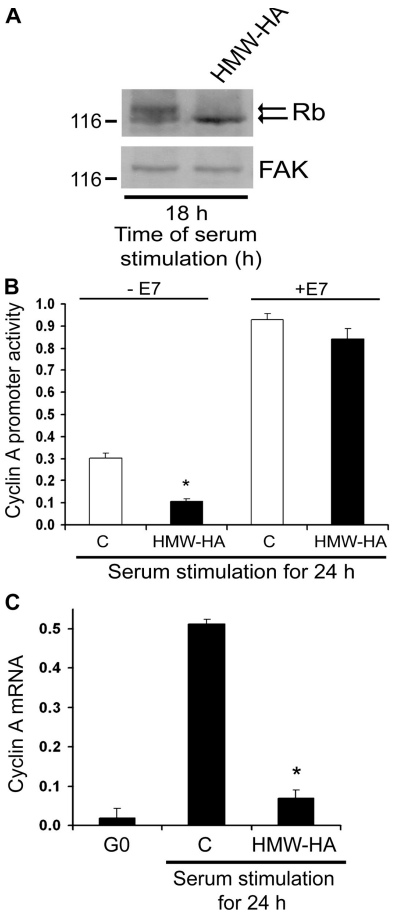

Figure 2. **Pocket protein–dependent effects of HMW-HA on cyclin A gene transcription.** Quiescent human vascular SMCs (G0) were stimulated with 10% FBS for the selected times in the absence (control, C) or presence of 200 μg/ml HMW-HA. (A) The cells were collected, lysed, and immunoblotted for Rb and focal adhesion kinase (FAK; loading control). Top and bottom arrows indicate the positions of hyper- and hypophosphorylated Rb, respectively. Quantification of Rb gel shifts from four independent experiments indicated that Rb phosphorylation after FBS stimulation (18–24 h) was 54 and 28% in the absence and presence of HMW-HA, respectively. (B) Human SMCs were cotransfected with plasmids encoding the cyclin A promoter-driving luciferase, empty vector or E7, and Renilla luciferase. The transfected cells were serum starved for 24 h and stimulated with 10% FBS. Cyclin A promoter activity was determined in the absence or presence of HMW-HA and E7. Cyclin A promoter-luciferase activity is normalized to Renilla luciferase activity. *, $P < 0.01$. (C) Quiescent (G0) human SMCs were stimulated with 10% FBS for 24 h. Total RNA was isolated and analyzed by QPCR for cyclin A mRNA and 18S rRNA. Cyclin A mRNA expression is normalized to 18S rRNA. *, $P < 0.001$. Error bars represent SD.

HMW-HA inhibits mitogen-dependent induction of the cyclin D1 and Skp2 genes

Cyclin D1–cdk4/6 and cyclin E–cdk2 are the G1-phase cdk complexes that are thought to control pocket protein phosphorylation. As discussed above (see Introduction), the rate-limiting step for the activation of these kinases is the mitogen-dependent induction of cyclin D1 (leading to active cyclin D–cdk4/6) and the depletion of cyclin/cdk2-bound p27 (leading to active cyclin E–cdk2). A time-course analysis showed that HMW-HA blocked both the mitogen-dependent induction of cyclin D1 and the mitogen-dependent down-regulation of p27 (Fig. 3 A). Cyclin D1 mRNA levels were inhibited by HMW-HA (Fig. 3 B), and the time course of this effect was similar to that seen for cyclin D1 protein (Fig. 3 A). In contrast, HMW-HA did not affect the levels of p27 mRNA (Fig. 3 C), indicating that its effect on p27 protein levels was likely posttranscriptional. These effects are selective because the mitogen-dependent changes in G1-phase p21 levels were unaffected by HMW-HA (Fig. 3 A).

The levels of p27 are typically controlled by ubiquitin-mediated degradation, and a major ubiquitin ligase responsible for degrading p27 is the multimeric complex called SCF^{Skp2} (Carrano et al., 1999; DeSalle and Pagano, 2001; Philipp-Staheli et al., 2001; Cardozo and Pagano, 2004). Mitogenic stimuli regulate the activity of SCF^{Skp2}, at least in large part, by controlling the expression of Skp2 (Pagano, 2004). We studied the effect of HMW-HA on Skp2 gene expression and found that the mitogen-dependent induction of Skp2 mRNA and protein were strongly inhibited by HMW-HA (Fig. 3 D).

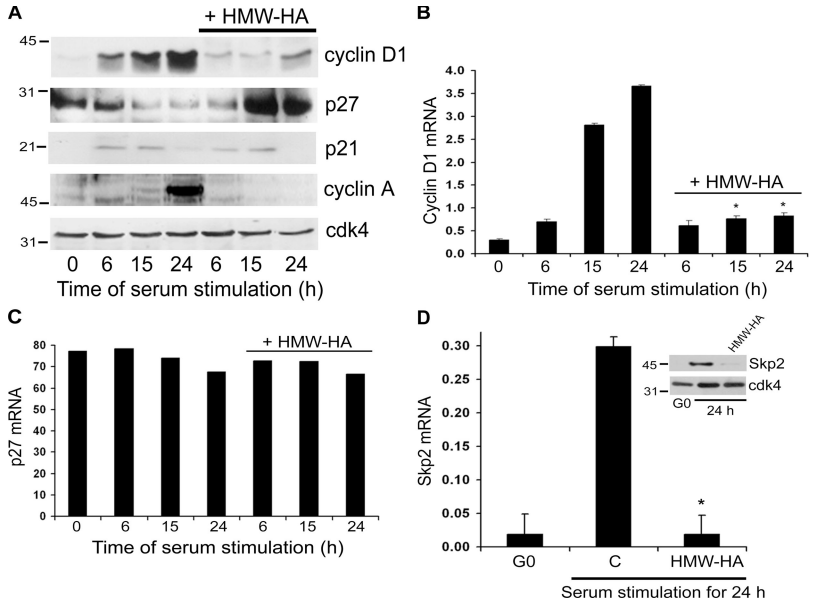

Figure 3. **Subcellular effects of HMW-HA on G1-phase cdks.** Quiescent human vascular SMCs (G0) were stimulated with 10% FBS for the selected times in the absence (control, C) or presence of 200 μg/ml HMW-HA. (A) Collected cells were lysed and immunoblotted for cyclin D1, p27, p21, cyclin A, and cdk4 (loading control). (B and C) Total RNA was isolated from SMCs and analyzed by QPCR for cyclin D1 mRNA, p27 mRNA, and 18S rRNA, and the levels of cyclin D1 (B) and p27 mRNA (C) were normalized to 18S rRNA. *, $P < 0.01$. (D) Quiescent human SMCs were stimulated with 10% FBS for 24 h in the absence or presence of 200 μg/ml HMW-HA. Total RNA was isolated from the SMCs and analyzed by QPCR for Skp2 mRNA and 18S rRNA. Skp2 mRNA expression is plotted relative to 18S rRNA. *, $P < 0.001$. Collected cells were also lysed and immunoblotted for Skp2 and cdk4 (inset). Error bars represent SD.

The combined results in Fig. 3 show that the antimitogenic effect of HMW-HA is associated with an inhibition of both cyclin D1 and Skp2 gene expression. Many studies have indicated that both of these effects would be expected to inhibit G1-phase progression and S-phase entry. Indeed, the ectopic expression of either cyclin D1 or Skp2 was sufficient to overcome the antimitogenic effect of HMW-HA on S-phase entry in vascular SMCs (Fig. 4 A).

Cyclin D1 is the primary target of HMW-HA

Recent studies indicate that Skp2 is an E2F target (Markey et al., 2002; Vernell et al., 2003; Zhang and Wang, 2006). This finding raised the possibility that cyclin D1 is the primary target of HMW-HA and that the inhibition of Skp2 seen in SMCs treated with HMW-HA is a secondary consequence of decreased cyclin D1–cdk4/6 activity, decreased Rb phosphorylation, and decreased E2F release (see Introduction). To determine whether the effects of HMW-HA on cyclin D1 and Skp2 are related or independent, we asked whether the ectopic expression of cyclin D1 would override the effect of HMW-HA on Skp2 gene expression. We found that the ectopic expression of cyclin D1 (Fig. 4 B) rescued the expression of Skp2 mRNA in HMW-HA–treated SMCs (Fig. 4 C). In contrast, the ectopic expression of Skp2 (Fig. 4 B) was unable to rescue cyclin D1 gene expression in the presence of HMW-HA (Fig. 4 D). The results from these experiments indicate that the primary antimitogenic effect of HMW-HA is on the expression of cyclin D1 and that the effect of HMW-HA on Skp2 is likely a secondary consequence of inhibiting cyclin D1–cdk4/6 complex formation, Rb phosphorylation, and E2F release.

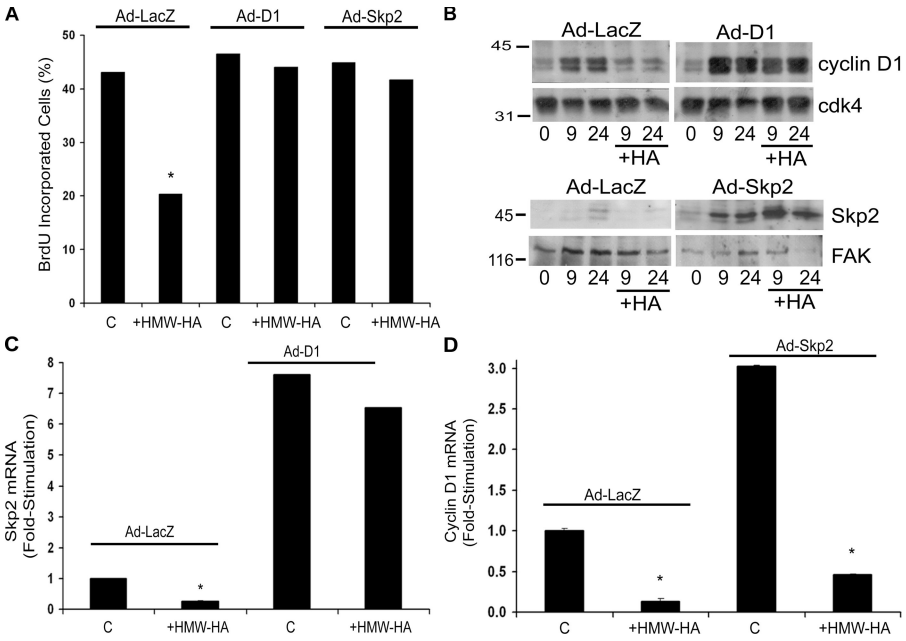

Figure 4. **Cyclin D1 is the proximal target of HMW-HA.** Human vascular SMCs infected with adenoviruses encoding lacZ (Ad-lacZ), cyclin D1 (Ad-D1), or Skp2 (Ad-Skp2) were serum starved and stimulated with 10% FBS-DME in the absence (control, C) or presence of 200 μg/ml HMW-HA. (A) The cultures were incubated for 24 h in the presence of BrdU, and BrdU incorporation into nuclei was determined by immunofluorescence microscopy. *, $P < 0.01$. (B) Collected cells were lysed and immunoblotted for cyclin D1 and cdk4 (loading control) or Skp2 and focal adhesion kinase (FAK; loading control). The thin vertical spaces between the Ad-lacZ, Ad-D1, and Ad-Skp2 images indicate reordering of these image blocks from the scanned gel. (C and D) Total RNA was isolated from the SMCs and used to determine the levels of Skp2 mRNA or cyclin D1 mRNA. The expression of cyclin D1 and Skp2 mRNAs was normalized to 18S rRNA and plotted relative to their expression levels in cells infected with the lacZ adenovirus. *, $P < 0.005$. Error bars represent SD.

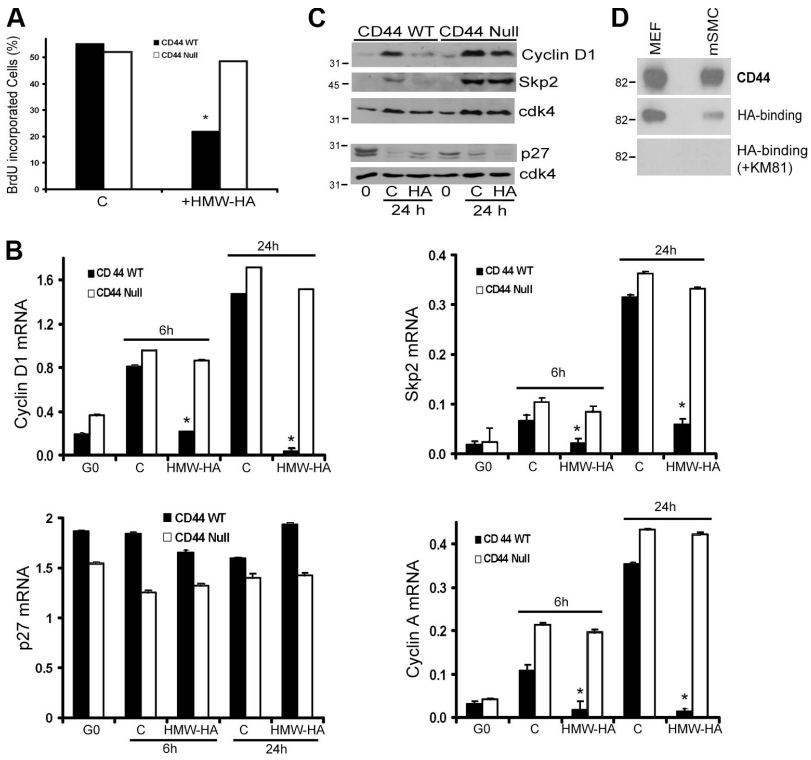

Figure 5. **HMW-HA inhibits cyclin D1, Skp2, and cyclin A expression in wild-type mouse vascular SMCs.** Quiescent (G0) mouse vascular SMCs from wild-type (WT) or CD44-null mice were stimulated with 10% FBS for the selected time intervals in the absence (control, C) or presence of 200 μg/ml HMW-HA. (A) Cells were incubated for 24 h in the presence of BrdU, and BrdU incorporation into nuclei was determined by immunofluorescence microscopy. *, $P < 0.002$. (B) Cells were collected, lysed, and analyzed by QPCR for cyclin D1, Skp2, cyclin A, and p27 mRNAs as well as for 18S rRNA. Results for each mRNA are plotted relative to 18S rRNA. *, $P < 0.01$. (C) Collected cells from identical experiments were analyzed by Western blotting for either cyclin D1, Skp2, and cdk4 (loading control) or p27 and cdk4 (loading control). (D) Primary MEFs and vascular SMCs were lysed and immunoblotted for CD44. HA binding to CD44 was determined using FITC-conjugated HA in the absence and presence of CD44-neutralizing antibody (KM81). Error bars represent SD.

Conserved effects of HA and CD44 on cyclin D1, Skp2, and cyclin A levels in primary mouse SMCs and fibroblasts

HMW-HA is antimitogenic in early passage mouse vascular SMCs, as determined by both BrdU incorporation (Fig. 5 A) and flow cytometry (Table I). Moreover, HMW-HA inhibits the mitogen-dependent induction of cyclin D1, Skp2, and cyclin A mRNAs (Fig. 5 B). The down-regulation of p27 was partially inhibited by HMW-HA in wild-type mouse SMCs (Fig. 5 C) without comparable change in the level of p27 mRNA (Fig. 5 B). Cyclin D1 and Skp2 proteins levels were also inhibited by HMW-HA (Fig. 5 C). All of these effects recapitulated the results we obtained in human SMCs.

The use of mouse SMCs allowed us to compare the effect of HMW-HA in wild-type and CD44-null cells. We found that none of the aforementioned HMW-HA effects were recapitulated in vascular SMCs isolated from CD44-null mice (Fig. 5, A–C). Thus, CD44 is the major HA receptor mediating the antimitogenic effects of HMW-HA in mouse vascular SMCs. Similar CD44-dependent effects of HMW-HA were detected in early passage mouse lung fibroblasts (Table II). Moreover, the ectopic expression of cyclin D1 overcame the inhibitory effects of HMW-HA on Skp2 mRNA, cyclin A mRNA, and S-phase entry in mouse embryonic fibroblasts (MEFs; Table III). Consistent with these results, HA binding to CD44 was detected in both primary mouse SMCs and fibroblasts (Fig. 5 D). Thus, the antimitogenic effects of HMW-HA and the critical role of CD44 in these effects are well conserved in mouse and human vascular SMCs as well as in mouse embryonic and lung fibroblasts.

Antimitogenic effects of CD44 on SMC mitogenesis in vivo

We then investigated whether CD44 regulates SMC mitogenesis in vivo. Aortae were isolated from 20-wk-old male wild-type and CD44-null mice, total RNA was isolated, and real-time quantitative PCR (QPCR) was performed to compare the levels of cyclin D1, Skp2, and cyclin A mRNAs. All three of these transcripts were increased in the aortae lacking CD44 (Fig. 6 A),

Table II. **Effects of HMW-HA on wild-type and CD44-null mouse lung fibroblasts**

	CD44 WT MLF		CD44-null MLF	
	−HMW-HA	+HMW-HA	−HMW-HA	+ HMW-HA
Cyclin D1 mRNA	0.37	0.07	0.39	0.36
Skp2 mRNA	0.27	0.04	0.26	0.24
Cyclin A mRNA	0.24	0.07	0.25	0.24
BrdU-incorporated cells (%)	43	21	42	38

Early passage adult mouse lung fibroblasts (MLFs) from wild-type (WT) or CD44-null mice were serum starved and stimulated with 10% FBS for 24 h in the absence (−) or presence (+) of 200 μg/ml HMW-HA. Total RNA was isolated, and QPCR was used to measure the levels of cyclin D1 mRNA, Skp2 mRNA, cyclin A mRNA, and 18S rRNA. The expression of cyclin D1, Skp2, and cyclin A mRNAs were normalized to 18S rRNA. Results show the means of duplicate PCR reactions. SDs ranged from 0.001 to 0.01. BrdU incorporation was determined 24 h after stimulation with 10% FBS.

Table III. **Cyclin D1 is the primary target of HMW-HA in early passage MEFs**

	Ad-lacZ		Ad-D1	
	−HMW-HA	+HMW-HA	−HMW-HA	+HMW-HA
Cyclin D1 mRNA	0.21	0.08	1.23	1.16
Skp2 mRNA	0.08	0.02	0.95	0.91
Cyclin A mRNA	0.11	0.01	0.22	0.24
BrdU-incorporated cells (%)	51	13	53	51

Near-confluent cultures of early passage MEFs were infected with adenoviruses encoding lacZ (Ad-lacZ) or cyclin D1 (Ad-D1) and were serum starved. Western blotting (unpublished data) confirmed overexpression of the proteins. The infected starved cells were incubated with 10% FBS and BrdU for 24 h in the absence (−) or presence (+) of 200 μg/ml HMW-HA. Total RNA was isolated, and QPCR was used to measure the levels of cyclin D1 mRNA, Skp2 mRNA, cyclin A mRNA, and 18S rRNA. The expression of cyclin D1, Skp2, and cyclin A mRNAs were normalized to 18S rRNA. QPCR results show the means of duplicate PCR reactions. SDs ranged from 0.001 to 0.007. BrdU incorporation was determined 24 h after stimulation with 10% FBS.

with fold increases of 6 ± 2.7 for cyclin D1, 8 ± 2.1 for Skp2, and 7.5 ± 1.5 for cyclin A mRNAs (mean ± SD; represents data from two pools of four aortae for a total of eight aortae). Cyclin D1 and Skp2 mRNA levels were also increased (relative to wild-type controls) in CD44-null aortic arches and thoracic aortae from 10-wk-old female mice (Fig. S1, available at http://www.jcb.org/cgi/content/full/jcb.200611058/DC1), indicating that these effects of CD44 are independent of age and gender. Note that the mRNA levels of CD31 (platelet endothelial cell adhesion molecule; endothelial marker), CD68 (macrophage marker), and smooth muscle actin (smooth muscle marker) were similar in the wild-type and CD44-null aortae, with smooth muscle actin being the most abundant as expected (Fig. 6 B). Thus, these CD44-dependent changes in cyclin D1, Skp2, and cyclin A mRNAs are not caused by alterations in the cellular composition of the samples. We conclude that in the uninjured artery, the binding of HMW-HA to CD44 exerts a negative effect on the cell cycle that helps to maintain arterial SMCs in a quiescent state in vivo.

Despite the increased expression of cyclin A mRNA, aortae isolated from CD44-null mice did not show gross evidence of SMC hyperplasia as assessed by morphometric analysis of hematoxylin and eosin– (Fig. 6 C, medial layer) or elastin (not depicted) -stained aortic sections. Thus, the increased expression of cyclin A mRNA in the CD44-null artery is apparently counterbalanced in vivo to maintain arterial homeostasis in the uninjured artery.

It is well established that intimal endothelial cells release potent antimitogens for underlying medial SMCs (see Discussion), and we reasoned that the release of these intimal antimitogens might be responsible for the absence of cell proliferation in resting CD44-null arteries (Fig. 6 C). Therefore, we denuded the endothelial layer of the femoral artery in wild-type and CD44-null mice by performing fine wire injuries. Although the intact endothelium is eventually restored after injury, the transient denudation results in proliferation of the medial SMCs, which can be detected by an increased intimal/medial ratio and BrdU labeling. We asked whether the loss of CD44 increased SMC proliferation in this injury setting.

Femoral arteries were isolated, fixed, and stained for elastin 14 d after arterial injury. The internal elastic lamina was restored in both wild-type and CD44-null mice (Fig. 7 A). However, neointimal thickening was clearly increased in the CD44-null mice relative to controls (Fig. 7 A). This proliferative effect was quantified by morphometric analysis, which showed an approximately twofold increase in the neointimal/medial

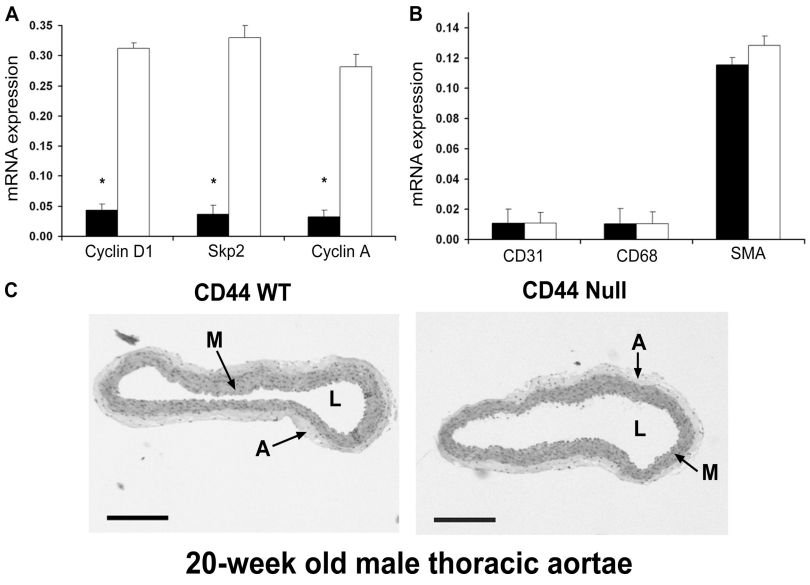

Figure 6. **CD44 regulates the expression of cyclin D1, Skp2, and cyclin A in the aorta.** (A and B) Total RNA was isolated twice from pooled, cleaned aortae of four 20-wk-old male CD44 wild-type (black bars) and CD44-null (white bars) mice for a total of eight mice/genotype. cDNA was synthesized for each isolation, and QPCR was performed on a cDNA aliquot for cyclin D1, Skp2, cyclin A mRNAs, and 18S rRNA (A) or CD31, CD68, smooth muscle actin (SMA) mRNAs, and 18S rRNA (B). The expression of cyclin D1, Skp2, cyclin A, CD31, CD68, and smooth muscle actin mRNAs are plotted relative to 18S rRNA. *, $P < 0.003$. Error bars represent SD. (C) Thoracic aortae were isolated from 20-wk-old male wild-type (WT) and CD44-null mice. The intima and adventitia were not removed before the tissues were fixed, embedded in paraffin, sliced in cross section, and stained with hematoxylin and eosin. Genotypes were confirmed by PCR. A, adventitia; M, media; L, lumen. Bars, 210 μm.

ratio (Fig. 7 B). A similar increase was seen in the number of BrdU-positive neointimal nuclei (Fig. 7 B). In contrast, neither wild-type nor CD44-null mice showed evidence of neointimal formation (Fig. 7 C) or SMC proliferation (not depicted) in sham-operated uninjured femoral arteries.

Discussion

Vascular SMCs synthesize HMW-HA, which is then released and deposited in the SMC matrix, where it can bind in an autocrine and paracrine fashion to the CD44 expressed on the SMC surface. We previously reported that the binding of HMW-HA to CD44 is antimitogenic for vascular SMCs (Cuff et al., 2001). Similarly, others have shown that HA inhibits PDGF-stimulated receptor activation and proliferation (Papakonstantinou et al., 1998; Li et al., 2006) and that the ectopic expression of HA synthases (which leads to the production of HMW-HA) inhibits the proliferation of arterial SMCs (Wilkinson, 2006).

The data presented here provide a mechanism for the antimitogenic effect of HMW-HA, show that this mechanism operates in vivo, and lead us to propose that the interaction between HA and CD44 on SMCs contributes to the maintenance of SMC quiescence in the healthy artery. First, our experiments with early passage human and mouse SMCs in culture show that HMW-HA can repress the mitogen-dependent induction of cyclin D1 and that this effect is associated with an inhibition of downstream cell cycle events such as Rb phosphorylation, Skp2 expression, p27 down-regulation, and cyclin A expression. Second, we show that the inhibitory effect of HMW-HA on cyclin D1 is causally related to its antimitogenic effect because ectopic cyclin D1 expression rescues S-phase entry in HMW-HA–treated cells.

In agreement with our results using vascular SMCs in culture, our data in vivo show that the expression of cyclin D1, Skp2, and cyclin A mRNAs is increased in the aortae of CD44-null mice, a result that strongly supports the physiological relevance of the HMW-HA effects we and others (Wilkinson, 2006) detect in vitro. The increased expression of cyclin A is typically associated with entry and progression through S phase, but resting aortae from CD44-null mice showed no gross evidence of SMC hyperplasia as compared with wild-type controls. There are several possible explanations for this result. First, increased proliferation of CD44-null SMCs could have been offset by increased turnover (Lakshman et al., 2005). Second, the lack of proliferation in CD44-null arterial SMCs could have reflected a compensatory change that occurs during development in the absence of CD44. Third, the intimal endothelium, which is known to release potent antimitogens such as TGF-β, nitric oxide, and prostacyclin (Cucina et al., 1998; Mombouli and Vanhoutte, 1999; Tanner et al., 2000), could have been obscuring the effect of CD44 deletion. Our ability to document the enhanced proliferation of CD44-null SMCs after arterial injury strongly supports the idea that the release of antimitogens from intact endothelium prevents the proliferation of medial SMCs in resting arteries of CD44-null mice.

HMW-HA is widely distributed in ECM in vivo, and our data indicate that the presence of HMW-HA provides an active, repressive signal that cooperates with intimal antimitogens to maintain vascular SMCs in a resting state. Our results also suggest that the degradation of HMW-HA to lower molecular weight forms, which is thought to occur at sites of arterial injury and inflammation (Noble, 2002), would eliminate the antimitogenic effects of HMW-HA and CD44. Additionally, the lower

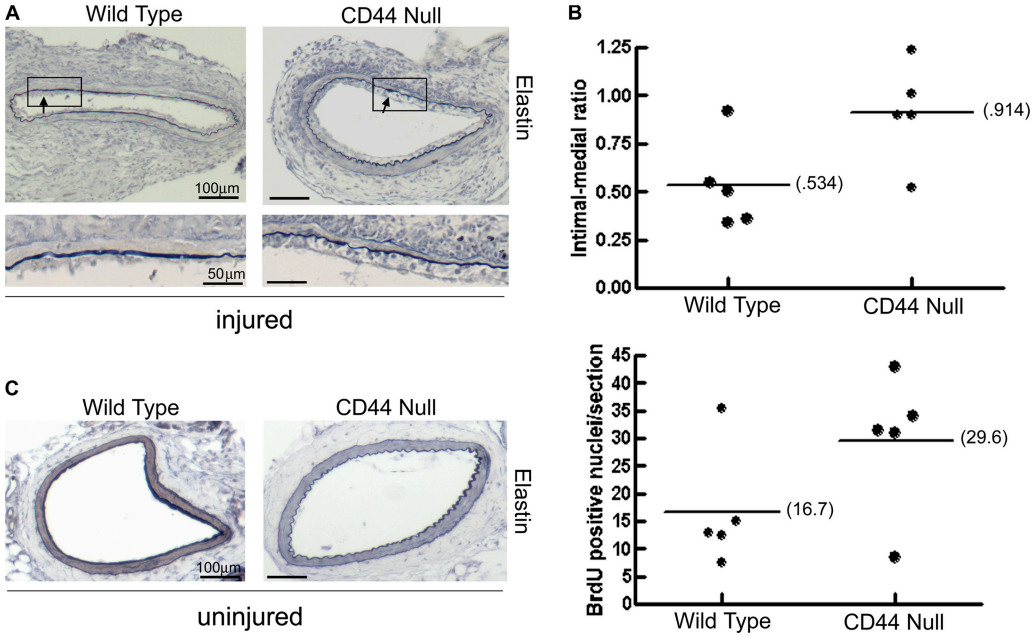

Figure 7. **Increased neointima formation and BrdU incorporation after vascular injury in CD44-null mice.** (A) Injured femoral arteries from wild-type and CD44-null mice were perfusion fixed, paraffin embedded, and sectioned before being stained for elastin. Boxes indicate the regions of the aortae that are shown at twofold higher magnification. Arrows indicate sites of neointima formation. (B) Intimal/medial ratios and the number of BrdU-positive nuclei in injured femoral arteries of wild-type and CD44-null mice. $n = 5$ per genotype. $P = 0.02$ for intimal/medial ratios, and $P = 0.06$ for BrdU as determined using a one-tailed *t* test. Horizontal bars indicate mean values. (C) The sham-operated control arteries from the mice in A were stained for elastin.

molecular forms of HA that may accumulate as a result of inflammation can exert a positive effect on G1-phase progression in and of themselves (Cuff et al., 2001; Nasreen et al., 2002; Huang et al., 2003). Together, the loss of HMW-HA and the appearance of its lower molecular weight isoforms could contribute to modulation of SMCs to the proliferative phenotype characteristic of vascular injury. Thus, we propose that the maintenance or degradation of HMW-HA can act as a rheostat, regulating the extent of growth factor– and ECM-dependent SMC proliferation.

Much of our study focused on the actions of HMW-HA on vascular SMCs so that we could assess molecular effects both in cultured cells and in vivo. However, we also show that HMW-HA is a potent antimitogenic factor for both lung and embryonic fibroblasts. In both primary SMCs and fibroblasts, the antimitogenic effect of HMW-HA is mediated by CD44. Moreover, HMW-HA similarly affects cyclin D1, Skp2, and p27 in SMCs and fibroblasts, and cyclin D1 is the primary target in both cell types. The broad distribution of HMW-HA and the expression of CD44 indicates that this ligand–receptor system is likely to have an antimitogenic effect on multiple mesenchymal cell types.

Materials and methods

Cell culture

Primary human vascular SMCs isolated from human aortae were obtained from Cascade Biologics, Inc., maintained as described previously (Motamed et al., 2002), and used between passage 2 and 9. Near-confluent monolayers were G0 synchronized by incubation in 1 mg/ml of serum-free DME containing heat-inactivated fatty acid–free BSA (DME-BSA) for 48 h. 14 mg/ml of a concentrated HMW-HA solution (Healon GV; GE Healthcare) was diluted to 200 μg/ml with DME and 10% FBS. The medium containing HMW-HA was then directly added to the quiescent cells. In some experiments, HMW-HA was supplemented with 1 μg/ml Polymyxin B (Sigma-Aldrich) to control for potential lipopolysaccharide contamination. As expected from our use of patient- grade HA, the addition of Polymyxin B had no effect on any of the results. Primary mouse vascular SMCs were isolated from aortae of wild-type and CD44-null C57BL/6 mice, maintained as described previously (Cuff et al., 2001), and used at passages 2–5. The adhesion and morphology of the wild-type and CD44-null SMCs were similar under the conditions of our experiments. Primary lung fibroblasts were isolated from 8–12-wk-old wild-type and CD44-null C57BL/6 mice. Primary MEFs were isolated from embryonic day 12.5 C57BL/6 embryos. The explanted mouse fibroblasts were maintained in DME containing 10% FBS and used at passage 2–5. Each of the fibroblast cell types was serum starved by incubation in DME-BSA for 48 h. To control for specificity, we tested the effect of exogenous heparan sulfate and found that it did not inhibit BrdU incorporation in serum-stimulated mouse or human SMCs.

Adenoviral infections and transfections

For adenoviral infections, 3×10^5 human vascular SMCs or 6×10^5 MEFs in 10% FBS-DME were seeded overnight in 100-mm dishes and incubated in DME-BSA for 12 h. Adenoviruses encoding lacZ, cyclin D1 (a gift from J. Albrecht, Hennepin County Medical Center, Minneapolis, MN), or Skp2 (a gift from K. Nakayama, Kyushu University, Fukuoka, Japan) were directly added to the near-confluent cultures and incubated overnight. The medium was then replaced with fresh DME-BSA, and the cultures were incubated for an additional 24 h. The infected starved cells were washed once with serum-free DME before being directly stimulated with 10% FBS in the presence or absence of 200 μg/ml HMW-HA. The adenovirally expressed cDNAs were efficiently expressed in the serum-stimulated but not serum-starved cells.

Cyclin A promoter-luciferase assays were performed after transient transfection of near-confluent SMCs (5×10^4 cells in 35-mm dishes) as described previously (Kothapalli et al., 2003) using 1 μg p434/cyclin A promoter-luciferase expression vector (bases −270–164), 0.01 μg Renilla luciferase vector, and 1 μg of either empty vector or an E7 expression vector. Cyclin A promoter-driven luciferase activity and Renilla luciferase activities were measured twice for each sample, and the mean ± SD was plotted.

Immunoblotting

Human or mouse vascular SMCs were seeded (3×10^5 cells per 100-mm dish), incubated overnight, serum starved, and stimulated with 10% FBS in the absence or presence of HMW-HA. The cells were then collected and lysed as described previously (Welsh et al., 2001). Total protein concentration was determined by Coomassie binding (Bio-Rad Laboratories). Equal amounts of protein (50–100 μg) were resolved on reducing SDS mini-gels and analyzed by immunoblotting using antibodies specific for the following proteins: cyclin D1, p21, cdk4 (all were obtained from Santa Cruz Biotechnology, Inc.), p27 (BD Transduction Laboratories), Skp2 (Zymed Laboratories), Rb (Zymed Laboratories), and COX-1 (Cayman Chemical). Rabbit polyclonal cyclin A antibody was prepared in our laboratory. The resolved proteins were detected using ECL (GE Healthcare). Autoradiograms were digitized by scanning, and figures were assembled using Photoshop (Adobe). The small numbers on the left side of each blot represent typical migration positions of molecular weight standards ($M_r \times 10^{-3}$).

Immunofluorescence microscopy

Human vascular SMCs, mouse vascular SMCs, mouse lung fibroblasts, and MEFs (70–80% confluent) were seeded on dishes containing autoclaved glass coverslips, serum starved, and stimulated with 10% FBS in the absence or presence of HMW-HA. In some experiments, 50 μg/ml of a species-specific blocking antibody to human CD44 (5F12; Liao et al., 1993) or an irrelevant isotype-matched antibody was added to the human SMCs at the time of FBS stimulation. Fixed cells were analyzed at room temperature by immunofluorescence for the incorporation of BrdU as described previously (Kothapalli et al., 2003) using AlexaFluor594-conjugated donkey anti–sheep secondary antibody to visualize BrdU staining. The percentage of BrdU-positive cells was assessed by epifluorescence microscopy by counting the number of BrdU-positive nuclei relative to the total number of DAPI-stained nuclei and typically counting ∼150 nuclei in several separate fields of view per sample. Stress fibers were stained using fluorescein-phalloidin as described previously (Welsh et al., 2001). Focal adhesions were immunostained using antivinculin (Sigma Aldrich) and AlexaFluor594-conjugated goat anti–mouse secondary antibody. A representative result is shown for each figure. Images were acquired using a microscope (Eclipse 80i; Nikon), 20× 0.45 NA plan Fluor (ELWD; Nikon) and 40× 0.7 NA PL Fluotar (Leitz) objectives, a digital camera (C4742-95; Hamamatsu), and a camera controller. Images were converted to TIFF files using Openlab imaging software (Improvision) and were assembled using Photoshop (Adobe).

Quantitative real-time RT-PCR

Quiescent human or mouse vascular SMCs were stimulated with 10% FBS in 100-mm dishes in the absence or presence of HMW-HA. The cells were washed once with cold PBS, scraped, and collected in 0.5 ml of fresh PBS. Total RNA was then extracted from the collected cell pellet using 1 ml TRIzol reagent (Invitrogen) followed by reverse transcription using ∼100 ng of total RNA as described previously (Stewart et al., 2004). An aliquot (10%) of the cDNA was subjected to PCR using TaqMan Universal PCR Master Mix (Applied Biosystems; Stewart et al., 2004). Real-time PCR for human cyclin D1 was performed using 900 nM of forward primer 5′-TGTTCGTGGCCTCTAAGATGAAG-3′, 900 nM of reverse primer 5′-AGGTTCCACTTGAGCTTGTTCAC-3′, and 250 nM of probe 5′-6FAM-AGCAGCTCCATTTGCAGCAGCTCCT-TAMRA-3′. Real-time PCR for mouse cyclin D1 was performed using 900 nM of forward primer 5′-TGCCATCCATGCGGAAA-3′, 900 nM of reverse primer 5′-AGCGGGAAGAACTCCTCTTC-3′, and 250 nM of probe 5′-6FAM-CTCACAGACCTCCAGCAT-MGBNFQ-3′. TaqMan gene expression assays (Applied Biosystems) were used to detect human Skp2 mRNA (assay ID Hs00261857_m1), human p27 (assay ID Hs00153277_m1), human cyclin A (assay ID Hs00171105_m1), mouse Skp2 (Stewart et al., 2004), mouse p27 (assay ID Mm00438167_g1), and mouse cyclin A (assay ID Mm00438064_m1). To detect both human and mouse 18S rRNA, we used TaqMan gene expression assay ID Hs99999901_s1 or 150 nM of forward primer 5′-CCTGGTTGATCCTGCCAGTAG-3′, 150 nM of reverse primer 5′-CCGTGCGTACTTAGACATGCA-3′, and 100 nM of probe VIC-TGCTTGTCTCAAAGATTA-MGB-NFQ. QPCR was performed as described previously using Taqman Universal PCR Master Mix (Stewart et al., 2004).

Each sample was analyzed in duplicate PCR reactions, and mRNA expression was quantified using ABI PRISM 7000 SDS software (Applied Biosystems). Mean quantities and SD were calculated from duplicate PCR reactions.

To perform QPCR on mouse arteries, aortae (excluding the abdominal aorta) were isolated from eight 20-wk-old male wild-type and CD44-null mice, both on the C57BL/6 background. After extensive cleaning to remove the adventitia and intima, the aortae were stabilized by submerging in RNALater (QIAGEN). Before isolating the total RNA, the aortae were weighed, and ~30 mg of aortic tissue (four aortae) were manually homogenized and treated with 20 mg/ml proteinase K (Roche Diagnostics) at 55°C for 10 m. The homogenate was clarified by centrifugation, and total RNA was isolated from the supernatant using RNeasy mini columns (QIAGEN). Reverse transcription and QPCR were performed as described in the previous paragraph using 20% of the reverse transcription reaction and primers and probes to mouse cyclin D1 mRNA, Skp2 mRNA, cyclin A mRNA, and 18S rRNA. Primers for mouse CD31 mRNA (forward 5′-CTGCAGGCATCGGCAAA-3′ and reverse 5′-GCATTTCGCACACCTGGAT-3′), mouse CD68 mRNA (forward 5′-TGGACAGCTTACCTTTGGATTCA-3′ and reverse 5′-TGTATTCCACCGCCATGTAGTC-3′), and mouse smooth muscle actin mRNA (forward 5′-CCAGAGCAAGAGAGGGATCCT-3′ and reverse 5′-TGTCGTCCCAGTTGGTGATG-3′) were obtained from Sigma-Genosys. The CD31, CD68, and smooth muscle actin mRNAs were analyzed using 1 μM of forward and reverse primers and SYBR Green PCR Master Mix (Applied Biosystems).

CD44 protein expression and HA binding

Near-confluent early passage primary MEFs or mouse vascular SMCs were lysed using 1.5% NP-40 in PBS containing a protease inhibitor cocktail (0.2 U/ml aprotinin and 0.2 mg/ml PMSF). Equal amounts of total protein were resolved on 7.5% SDS gels under nonreducing conditions and transferred to polyvinylidene difluoride membranes. Proteins were analyzed by immunoblotting with an antibody (KM81) that detects total mouse CD44. HA binding to CD44 was detected by incubating the polyvinylidene difluoride membranes with FITC-HA in the presence or absence of blocking anti-CD44 (KM81; Miyake et al., 1990). Total CD44 levels and HA binding were visualized by ECL using HRP-conjugated secondary anti–rat IgG (Jackson ImmunoResearch Laboratories) and anti-FITC (Roche Diagnostics), respectively.

Femoral artery injury

The intimal layer of the left femoral artery was denuded in anesthetized wild-type and CD44-null C57BL/6 male mice (24–28 wk and 30–32 g) by insertion of a 0.36-mm angioplasty guide wire (Advanced Cardiovascular Systems) largely as described previously (Roque et al., 2000) except that the anesthesia was avertin, and the guide wire was kept in the femoral artery for 3 min. The right femoral artery was sham operated and used as control. The mice were maintained on a standard diet and water ad libitum. 14 d after injury, the mice were anesthetized, perfused with 0.9% NaCl (by placement of a 22-gauge needle in the left ventricle), and perfusion fixed in situ by infusion with Prefer fixative (Anatech Ltd.). In some experiments, the mice received four injections of 50 mg/kg BrdU intraperitoneally 12, 24, 48, and 72 h before perfusion. Both right and left femoral arteries were harvested and embedded in paraffin. All procedures were approved and animal husbandry was overseen by the Institutional Animal Care and Usage Committee of the University of Pennsylvania.

5-μm cross sections were made through the injured part of the isolated femoral artery, and identical cross sections were made in the sham-operated arteries. Three sections corresponding to the peak injury region of each artery were processed for elastin staining using the Accustain Elastic Stain (Sigma-Aldrich). Adjacent sections were stained with BrdU Labeling and Detection Kit II (Roche Diagnostics) according to manufacturer's instructions except that we first performed HCl-trypsin antigen retrieval generally as described previously (Cheng et al., 2002), incubated the sections in NH_4Cl, and blocked them with 20 mg/ml BSA in PBS. Images of the elastin- and anti-BrdU–stained sections were captured using a microscope (Eclipse 80i; Nikon), 10× 0.3 NA plan Fluor or 20× 0.45 NA plan Fluor objectives (Nikon), and a color camera (MicroPublisher 5.0 RTV; QImaging). Each of the elastin-stained sections were subjected to a morphometric analysis with Openlab software (Improvision) to determine mean intimal and medial areas (Roque et al., 2000). The total number of BrdU-positive nuclei in a peak injury section was determined by visual counting of the captured image. Samples showing the highest and lowest injury responses for each genotype were removed from the analysis, and the remaining data were plotted using Prism software (GraphPad). Statistical analysis used the one-tailed unpaired *t* test.

Online supplemental material

Fig. S1 shows the effect of CD44 on cyclin D1 and Skp2 mRNA in female mice. Online supplemental material is available at http://www.jcb.org/cgi/content/full/jcb.200611058/DC1.

We thank Jeffrey Albrecht and Keiichi Nakayama for adenoviruses.

This work was supported by National Institutes of Health grant HL62250.

Submitted: 10 November 2006
Accepted: 3 January 2007

References

Aruffo, A., I. Stamenkovic, M. Melnick, C.B. Underhill, and B. Seed. 1990. CD44 is the principal cell surface receptor for hyaluronate. *Cell*. 61:1303–1313.

Bagui, T.K., S. Mohapatra, E. Haura, and W.J. Pledger. 2003. P27Kip1 and p21Cip1 are not required for the formation of active D cyclin-cdk4 complexes. *Mol. Cell. Biol.* 23:7285–7290.

Banerji, S., J. Ni, S.X. Wang, S. Clasper, J. Su, R. Tammi, M. Jones, and D.G. Jackson. 1999. LYVE-1, a new homologue of the CD44 glycoprotein, is a lymph-specific receptor for hyaluronan. *J. Cell Biol.* 144:789–801.

Bono, P., K. Rubin, J.M. Higgins, and R.O. Hynes. 2001. Layilin, a novel integral membrane protein, is a hyaluronan receptor. *Mol. Biol. Cell*. 12:891–900.

Bradshaw, A.D., and E.H. Sage. 2001. SPARC, a matricellular protein that functions in cellular differentiation and tissue response to injury. *J. Clin. Invest.* 107:1049–1054.

Brown, T.A., T. Bouchard, T. St John, E. Wayner, and W.G. Carter. 1991. Human keratinocytes express a new CD44 core protein (CD44E) as a heparan-sulfate intrinsic membrane proteoglycan with additional exons. *J. Cell Biol.* 113:207–221.

Cardozo, T., and M. Pagano. 2004. The SCF ubiquitin ligase: insights into a molecular machine. *Nat. Rev. Mol. Cell Biol.* 5:739–751.

Carrano, A.C., E. Eytan, A. Hershko, and M. Pagano. 1999. SKP2 is required for ubiquitin-mediated degradation of the CDK inhibitor p27. *Nat. Cell Biol.* 1:193–199.

Cheng, Y., S.C. Austin, B. Rocca, B.H. Koller, T.M. Coffman, T. Grosser, J.A. Lawson, and G.A. FitzGerald. 2002. Role of prostacyclin in the cardiovascular response to thromboxane A2. *Science*. 296:539–541.

Cucina, A., A.V. Sterpetti, V. Borrelli, S. Pagliei, A. Cavallaro, and L.S. D'Angelo. 1998. Shear stress induces transforming growth factor-beta 1 release by arterial endothelial cells. *Surgery*. 123:212–217.

Cuff, C.A., D. Kothapalli, I. Azonobi, S. Chun, Y. Zhang, R. Belkin, C. Yeh, A. Secreto, R.K. Assoian, D.J. Rader, and E. Puré. 2001. The adhesion receptor CD44 promotes atherosclerosis by mediating inflammatory cell recruitment and vascular cell activation. *J. Clin. Invest.* 108:1031–1040.

DeSalle, L.M., and M. Pagano. 2001. Regulation of the G1 to S transition by the ubiquitin pathway. *FEBS Lett.* 490:179–189.

Dimova, D.K., and N.J. Dyson. 2005. The E2F transcriptional network: old acquaintances with new faces. *Oncogene*. 24:2810–2826.

Fraser, J.R., T.C. Laurent, and U.B. Laurent. 1997. Hyaluronan: its nature, distribution, functions and turnover. *J. Intern. Med.* 242:27–33.

Greenfield, B., W.C. Wang, H. Marquardt, M. Piepkorn, E.A. Wolff, A. Aruffo, and K.L. Bennett. 1999. Characterization of the heparan sulfate and chondroitin sulfate assembly sites in CD44. *J. Biol. Chem.* 274:2511–2517.

Hawkins, C.L., and M.J. Davies. 1998. Degradation of hyaluronic acid, poly- and monosaccharides, and model compounds by hypochlorite: evidence for radical intermediates and fragmentation. *Free Radic. Biol. Med.* 24:1396–1410.

Huang, L., Y.Y. Cheng, P.L. Koo, K.M. Lee, L. Qin, J.C. Cheng, and S.M. Kumta. 2003. The effect of hyaluronan on osteoblast proliferation and differentiation in rat calvarial-derived cell cultures. *J. Biomed. Mater. Res. A*. 66:829–839.

Kothapalli, D., S.A. Stewart, E.M. Smyth, I. Azonobi, E. Puré, and R.K. Assoian. 2003. Prostacylin receptor activation inhibits proliferation of aortic smooth muscle cells by regulating cAMP response element-binding protein- and pocket protein-dependent cyclin a gene expression. *Mol. Pharmacol.* 64:249–258.

Lakshman, M., V. Subramaniam, S. Wong, and S. Jothy. 2005. CD44 promotes resistance to apoptosis in murine colonic epithelium. *J. Cell. Physiol.* 203:583–588.

Li, L., C.-H. Heldin, and P. Heldin. 2006. Inhibition of platelet-derived growth factor-BB-induced receptor activation and fibroblast migration by hyaluronan activation of CD44. *J. Biol. Chem.* 281:26512–26519.

Liao, H.X., M.C. Levesque, K. Patton, B. Bergamo, D. Jones, M.A. Moody, M.J. Telen, and B.F. Haynes. 1993. Regulation of human CD44H and CD44E isoform binding to hyaluronan by phorbol myristate acetate and anti-CD44 monoclonal and polyclonal antibodies. *J. Immunol.* 151:6490–6499.

Markey, M.P., S.P. Angus, M.W. Strobeck, S.L. Williams, R.W. Gunawardena, B.J. Aronow, and E.S. Knudsen. 2002. Unbiased analysis of RB-mediated transcriptional repression identifies novel targets and distinctions from E2F action. *Cancer Res*. 62:6587–6597.

Miyake, K., K.L. Medina, S. Hayashi, S. Ono, T. Hamaoka, and P.W. Kincade. 1990. Monoclonal antibodies to Pgp-1/CD44 block lympho-hemopoiesis in long-term bone marrow cultures. *J. Exp. Med.* 171:477–488.

Mombouli, J.V., and P.M. Vanhoutte. 1999. Endothelial dysfunction: from physiology to therapy. *J. Mol. Cell. Cardiol.* 31:61–74.

Motamed, K., S.E. Funk, H. Koyama, R. Ross, E.W. Raines, and E.H. Sage. 2002. Inhibition of PDGF-stimulated and matrix-mediated proliferation of human vascular smooth muscle cells by SPARC is independent of changes in cell shape or cyclin-dependent kinase inhibitors. *J. Cell. Biochem.* 84:759–771.

Murphy-Ullrich, J.E. 2001. The de-adhesive activity of matricellular proteins: is intermediate cell adhesion an adaptive state? *J. Clin. Invest.* 107:785–790.

Nasreen, N., K.A. Mohammed, J. Hardwick, R.D. Van Horn, K. Sanders, H. Kathuria, F. Loghmani, and V.B. Antony. 2002. Low molecular weight hyaluronan induces malignant mesothelioma cell (MMC) proliferation and haptotaxis: role of CD44 receptor in MMC proliferation and haptotaxis. *Oncol. Res.* 13:71–78.

Noble, P.W. 2002. Hyaluronan and its catabolic products in tissue injury and repair. *Matrix Biol.* 21:25–29.

Pagano, M. 2004. Control of DNA synthesis and mitosis by the Skp2-p27-Cdk1/2 axis. *Mol. Cell*. 14:414–416.

Papakonstantinou, E., M. Roth, L.-H. Block, V. Mirtsou-Fidani, P. Argiriadis, and G. Karakiulakis. 1998. The differential distribution of hyaluronic acid in the layers of human atheromatic aortas is associated with vascular smooth muscle cell proliferation and migration. *Atherosclerosis*. 138:79–89.

Philipp-Staheli, J., S.R. Payne, and C.J. Kemp. 2001. p27(Kip1): regulation and function of a haploinsufficient tumor suppressor and its misregulation in cancer. *Exp. Cell Res.* 264:148–168.

Puré, E., and C.A. Cuff. 2001. A crucial role for CD44 in inflammation. *Trends Mol. Med.* 7:213–221.

Roque, M., J.T. Fallon, J.J. Badimon, W.X. Zhang, M.B. Taubman, and E.D. Reis. 2000. Mouse model of femoral artery denudation injury associated with the rapid accumulation of adhesion molecules on the luminal surface and recruitment of neutrophils. *Arterioscler. Thromb. Vasc. Biol.* 20:335–342.

Sherr, C.J., and J.M. Roberts. 1999. CDK inhibitors: positive and negative regulators of G1 phase progression. *Genes Dev.* 13:1501–1512.

Stamenkovic, I., A. Aruffo, M. Amiot, and B. Seed. 1991. The hematopoietic and epithelial forms of CD44 are distinct polypeptides with different adhesion potentials for hyaluronate-bearing cells. *EMBO J.* 10:343–348.

Stewart, S.A., D. Kothapalli, Y. Yung, and R.K. Assoian. 2004. Antimitogenesis linked to regulation of Skp2 gene expression. *J. Biol. Chem.* 279:29109–29113.

Tanner, F.C., P. Meier, H. Greutert, C. Champion, E.G. Nabel, and T.F. Luscher. 2000. Nitric oxide modulates expression of cell cycle regulatory proteins: a cytostatic strategy for inhibition of human vascular smooth muscle cell proliferation. *Circulation*. 101:1982–1989.

Turley, E.A., D. Moore, and L.J. Hayden. 1987. Characterization of hyaluronate binding proteins isolated from 3T3 and murine sarcoma virus transformed 3T3 cells. *Biochemistry*. 26:2997–3005.

Vernell, R., K. Helin, and H. Muller. 2003. Identification of target genes of the p16INK4A-pRB-E2F pathway. *J. Biol. Chem*. 278:46124–46137.

Welsh, C.F., K. Roovers, J. Villanueva, Y. Liu, M.A. Schwartz, and R.K. Assoian. 2001. Timing of cyclin D1 expression within G1 phase is controlled by Rho. *Nat. Cell Biol.* 3:950–957.

Wilkinson, T.S., S.L. Bressler, S.P. Evanko, K.R. Braun, and T.N. Wight. 2006. Overexpression of hyaluronan synthases alters vascular smooth muscle cell phenotype and promotes monocyte adhesion. *J. Cell. Physiol*. 206:378–385.

Zhang, L., and C. Wang. 2006. F-box protein Skp2: a novel transcriptional target of E2F. *Oncogene*. 25:2615–2627.